

Radiation Electrochemistry of the Colloidal Cadmium Microelectrode. Catalysis of Hydrogen Formation by Organic Free Radicals

A. Henglein* and J. Lilie

Hahn-Meitner-Institut für Kernforschung Berlin GmbH, Bereich Strahlenchemie, D-1000 Berlin 39, Postfach, West Germany

(Received: December 1, 1980)

Cadmium sols with a mean particle size of 11 nm or less were obtained in the radiolytic reduction of Cd^{2+} ions in the presence of 10^{-4} – 10^{-3} base-M sodium polyvinyl sulfate. These sols which contained small concentrations of residual Cd^{2+} were found to catalyze the formation of hydrogen by 1-hydroxy-1-methylethyl radicals, $(\text{CH}_3)_2\text{COH}$, as efficiently as the sols of the previously studied noble metals. The organic radicals transfer electrons to the colloidal particles at a practically diffusion-controlled rate. The cathodically charged colloidal particles first reduce and deposit residual cadmium ions and then store excess electrons. Both the stored electrons and the deposited cadmium atoms are able to produce H_2 from water. The reduction of water by deposited cadmium atoms is explained by a two-step mechanism: (1) dissolution of an atom as Cd^{2+} to leave negative charges on the colloidal particle and (2) transfer of these charges to water. The mechanism of catalysis is also described in terms of an equivalent electrical circuit, in which the colloidal microelectrode appears as a capacitance for the storage of reduction equivalents. A 3×10^{-4} M cadmium solution (containing $\sim 3 \times 10^{-5}$ M residual Cd^{2+} ions) was found to have a capacity of 0.98 F/L for the storage of excess electrons.

1. Introduction

Noble metals in the colloidal state have recently been shown to catalyze the formation of hydrogen by organic free radicals in aqueous solution.¹⁻⁵ In this catalytic reaction, the colloidal metals act as microelectrodes that are cathodically charged by electrons picked up from the radicals until the reduction of water takes place. Methods have been developed to determine the rate of electron transfer from the radicals to the colloidal particles, the rate of reduction of water by the stored electrons, the specific capacity of the microelectrodes, and the chemical potential of the stored electrons, i.e., to characterize such microelectrodes and their reactions in the same way as for compact electrodes in electrochemistry.^{4,5}

The more electronegative base metals have not yet been used as catalysts of free-radical reactions. Aside from the difficulties encountered in the preparation of colloidal solutions of such metals, a simple thermodynamic consideration of which of these metals should redissolve may make one reject the idea of using them as colloidal catalysts in aqueous solutions. Nevertheless, the preparation of slightly acidic colloidal solutions of cadmium, whose standard potential is as negative as -0.403 V, is reported in the present paper, and it is also shown that these solutions exhibit interesting catalytic activities. The stability of such colloids of cadmium is due to its large overpotential for the evolution of hydrogen from water.⁶ In fact, when colloidal cadmium is used as a storage system for electrons, the dissolution of the metal is even more effectively retarded; i.e., the lifetime of the catalyst increased. (On first sight, it may appear surprising that a catalyst is protected by using it intently instead of keeping it carefully stored.)

2. Experimental Section

2.1. Preparation of Cadmium Sols. The sols were prepared by chemically reducing cadmium ions with ra-

diation in the presence of sodium polyvinyl sulfate (PVS) as a stabilizer. The main reducing species generated in the γ irradiation of aqueous solutions is the hydrated electron. It is known to produce Cd^+ ions from Cd^{2+} , and cadmium metal is known to be formed in subsequent agglomeration processes.⁷ A complication arises from the oxidizing OH radicals that are simultaneously formed by the ionizing radiation. When OH-radical scavengers such as sodium formate or 2-propanol are added, new radicals, i.e., CO_2^- or $(\text{CH}_3)_2\text{COH}$, respectively, are formed, which also influence the rate of the cadmium reduction. It is known that the yield of cadmium precipitated in the absence of PVS is lower in the presence of 2-propanol ($G(\text{Cd}) = 0.4/100$ eV) than in the presence of sodium formate ($G(\text{Cd}) = 1.3$).⁷ The color of the cadmium sol in the presence of PVS depended on the nature of the OH-radical scavenger as well as on the dose rate applied. The "formate sol" had a yellow-green color with a grey tinge when it was formed at dose rates of several 10^5 rd/h. It was blue or violet when it was produced at low dose rates of some 10^4 rd/h. The "alcohol sol" was blue at all dose rates applied.

The solution contained cadmium perchlorate at a concentration of 3×10^{-4} M or less. PVS was present at a concentration of 10^{-4} – 10^{-3} base-M (mol wt of PVS: 65000). The concentration of the OH scavenger was 3.0×10^{-3} M in the case of sodium formate and 0.2 M in the case of 2-propanol. The solution was outgassed by evacuating first with a water pump and then with a high-vacuum diffusion pump. The Pyrex vessel carried an optical cell or a conductivity cell. The optical and conductometric measurements could thus be carried out without exposure of the irradiated solution to air. After an absorbed dose of $\sim 3 \times 10^5$ rd/h, the formation of the colloid was completed. The solution was again evacuated in order to remove the radiolytically formed hydrogen. All of the following procedures to use the solution as a catalyst had to be carried out under careful exclusion of air as the colloidal cadmium was dissolved within seconds upon contact with oxygen.

2.2. Measurement of Hydrogen Yields. In order to investigate the formation of H_2 by 1-hydroxy-1-methylethyl

(1) Henglein, A. *J. Phys. Chem.* 1979, 83, 2209-16.

(2) Meisel, D. *J. Am. Chem. Soc.* 1979, 101, 6133-5.

(3) Kiwi, J.; Grätzel, M. *J. Am. Chem. Soc.* 1979, 101, 7214-7.

(4) Henglein, A.; Lilie, J. *J. Am. Chem. Soc.* 1981, 103, 1059-66.

(5) Westerhausen, J.; Henglein, A.; Lilie, J. *Ber. Bunsenges. Phys. Chem.* 1981, 85, 182-9.

(6) Vetter, K. J. "Elektrochemische Kinetik"; Springer-Verlag, West Berlin 1961, p 467.

(7) Kelm, M.; Lilie, J.; Henglein, A. *J. Chem. Soc., Faraday Trans. 1*, 1975, 71, 1132-42.

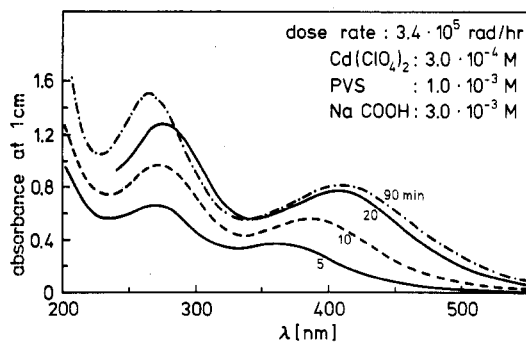


Figure 1. Absorption spectrum of a formate-cadmium perchlorate-sodium polyvinyl sulfate solution at various times of γ irradiation at a dose rate of 3.4×10^5 rd/h.

radicals, $(\text{CH}_3)_2\text{COH}$, 0.1 M acetone and 0.2 M 2-propanol were added to the formate sol. Upon γ irradiation of a solution containing acetone and 2-propanol, 1-hydroxy-1-methylethyl radicals are formed with a yield of six radicals per 100 eV of absorbed radiation energy. The total hydrogen yield observed, minus the yield of 1.04 H₂ molecules/100 eV produced in the absence of the cadmium, is designated as "excess hydrogen yield". The gas was collected by a Toepler pump, and the amount determined in a McLeod manometer.

2.3. Conductivity Measurements. In order to follow the reduction of Cd²⁺ during the preparation of the sol, we measured the increase in conductivity with a commercial conductometric bridge. Such measurements were only carried out with the alcohol sols which did not contain any buffering substance.

The transfer of electrons from 1-hydroxy-1-methylethyl radicals to the colloidal particles is accompanied by the formation of protons. This reaction can therefore be traced by the corresponding increase in conductivity of the solution. The rate was determined by conductometric pulse radiolysis using the sensitive detection technique that allows one to work at radical concentrations of 10^{-8} M.⁴ Such low concentrations had to be used in order to avoid radical-radical reactions besides the desired radical-colloid reaction.

The transfer of electrons from the colloid to the aqueous solvent is accompanied by a consumption of protons. Stationary-state measurements upon continuous irradiation with weak pulses of high-energy electrons (each pulse producing radicals at some 10^{-8} M) were carried out as has previously been described in detail.⁴ In the stationary state, the rates of electron transfer from the radicals to the colloid and from the colloid to water are equal, and the conductivity signal reaches a constant value. When the radiation was turned off, the conducting signal decreased, and the nature of the electron transfer from the colloid to water could be elucidated from this decrease.

3. Experimental Results

3.1. Formation and Spectra of the Sols. Figures 1 and 2 show how the optical spectra of the "formate" and the "alcohol sol" developed during γ irradiation at a dose rate of 3.4×10^5 rd/h. The spectrum of the formate sol contained two absorption maxima at 270 and 412 nm. In the earlier stages of irradiation, the second maximum appeared at wavelengths shorter than 412 nm. After 40 min, the spectrum did not change upon further irradiation. The alcohol sol also possessed two bands. The band in the near-UV, however, was less pronounced, and the band at long wavelengths was stronger and broader than that of the formate sol. One may suppose from these observations that the formate sol contained particles of smaller size and

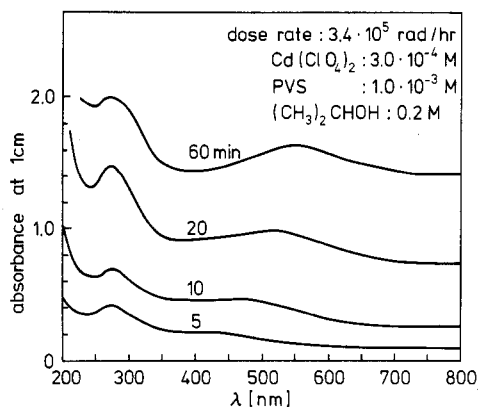


Figure 2. Absorption spectrum of a 2-propanol-cadmium perchlorate-sodium polyvinyl sulfate solution at various times of γ irradiation at a dose rate of 3.4×10^5 rd/h.

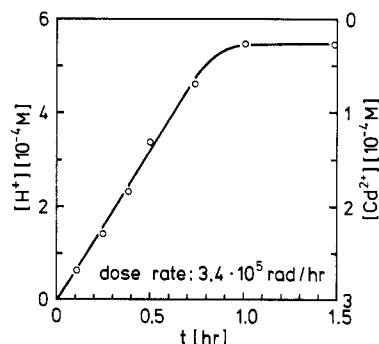


Figure 3. Concentration of hydrogen ions as a function of time. Irradiated solution: 3.0×10^{-4} M Cd(ClO₄)₂, 5×10^{-4} M PVS, and 0.2 M 2-propanol.

of a more narrow size distribution than the alcohol sol.

The absorbance of the sols (3×10^{-4} M cadmium) decreased upon thermal aging by $\sim 2\%$ per day. The decrease was slower when the sols were continuously γ -irradiated after the addition of acetone and 2-propanol, i.e., under the conditions where reducing radicals were produced.

Figure 3 shows the increase in the concentration of hydrogen ions during the formation of the alcohol sol. Two protons are formed per Cd²⁺ ion reduced. The right-hand ordinate gives the calculated concentration of Cd²⁺ ions. A yield of 1.8 protons/100 eV or 0.9 cadmium atom formed per 100 eV is calculated from the initial slope of the curve. The hydrogen-ion concentration reached a plateau after ~ 1 h, which was close to but distinctly below the maximum value of 6.0×10^{-4} M that would correspond to the complete reduction of the Cd²⁺ ions. While the slope of the straight line at short times was quite reproducible, the plateau at longer times reached different values between 4.2×10^{-4} and 5.5×10^{-4} M for various batches. As mentioned in the Introduction, one cannot expect the sol of an electronegative metal to exist for a long time without partial dissolution. At Cd²⁺ concentrations of a few 10^{-5} M, the rate of dissolution apparently is so slow that the cadmium sol is stable, at least for minutes or hours, i.e., the time taken for the experiments after its formation.

3.2. Catalysis of Hydrogen Formation. Figure 4 shows the amount of excess hydrogen produced in the irradiation of the acetone plus 2-propanol containing formate sol. The longest irradiation time in these experiments exceeded 2 weeks. A yield of 2.1 molecules of H₂ per 100 eV is calculated from the slope of the straight line obtained. This yield is as high as in the irradiation of colloidal silver solutions.¹

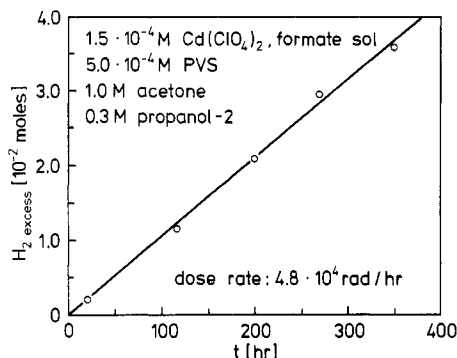


Figure 4. Amount of excess hydrogen produced in the irradiation of 1 L of the acetone-2-propanol-formate sol as a function of the irradiation time.

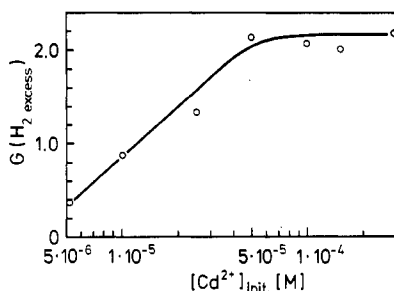


Figure 5. Yield of excess hydrogen as a function of the initial concentration of $\text{Cd}(\text{ClO}_4)_2$ used in the preparation of the formate sol. Dose rate: 4.7×10^6 rd/h.

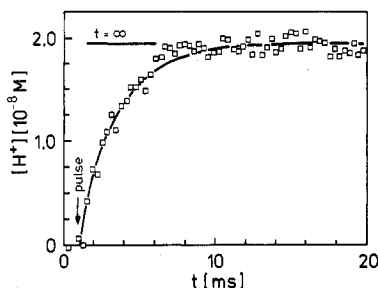


Figure 6. Buildup in H^+ concentration after a short pulse of high-energy electrons. Average over 16 pulses, each of which produced 2×10^{-8} M concentration of radicals. $t = \infty$: assumed final H^+ concentration for the calculated first-order curve. Alcohol sol with 3.0×10^{-4} M cadmium.

The dependence of the yield of excess hydrogen on the concentration of the cadmium in the formate sol is shown by Figure 5. It can be recognized that the maximum yield was still observed at a concentration as low as 5×10^{-5} M. Below this concentration, the yield became smaller. High yields of hydrogen were also obtained when the concentration of PVS was decreased to 10^{-4} base-M.

3.3. Rate of Electron Transfer from 1-Hydroxy-1-methylethyl Radicals to Colloidal Cadmium. Figure 6 shows a typical computer graph for the increase in conductivity of an acetone-containing alcohol sol as a function of time after the application of a pulse of high-energy electrons. On the ordinate axis, the concentration of protons formed is given. The points are averaged over 16 pulses each of which produced 1-hydroxy-2-methylethyl radicals at a concentration of 2.0×10^{-8} M. The time interval between the pulses was 0.3 s. The curve in Figure 6 was computer calculated for a first-order process. Its shape did not change when weaker pulses were applied. The half-life of the increase in conductivity was 2.0×10^{-3} s. In the absence of the colloid, i.e., in the presence of Cd^{2+} ions only, no change in conductivity was observed.

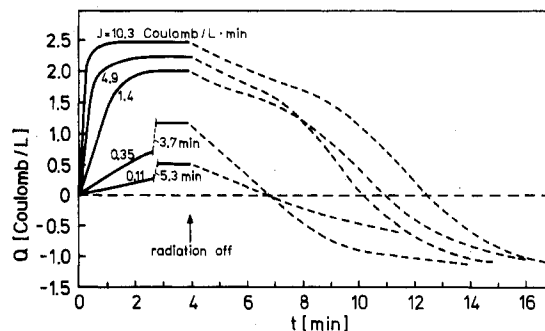


Figure 7. Stored reduction equivalents in an alcohol sol during irradiation (full line) and after irradiation (dashed line). The dose rates were 1.4×10^6 , 6.9×10^5 , 2.0×10^5 , 1.5×10^4 , and 4.9×10^4 rd/h, respectively.

The increase in conductivity is attributed to the electron transfer from the organic radicals to colloidal particles of cadmium (eq 1, where n = agglomeration number).



The observed half-life $\tau_{1/2}$ of the process may now be used to calculate an upper value for the radius of the colloidal particles, assuming that reaction 1 occurs at a diffusion-controlled rate. This assumption is not implausible as it has been shown that other colloidal metals such as silver and gold react with 1-hydroxy-1-methylethyl radicals at practically every encounter.^{4,5} The rate constant of a diffusion-controlled reaction between a small molecule and a large colloidal particle is

$$k = 4\pi NRd/1000 \quad (2)$$

where R is the radius of the colloidal particle, d is the diffusion coefficient of the radical, and $N = 6.03 \times 10^{23}$. The rate $k[\text{Cd}_n]$ of the reaction is given by eq 3. When

$$k[\text{Cd}_n] = \ln 2/\tau_{1/2} \quad (3)$$

C_0 is the overall concentration of reduced cadmium, one obtains eq 4. Assuming that the colloidal particles are

$$[\text{Cd}_n] = C_0/n \quad (4)$$

spherical and have the density of 8.64 g cm^{-3} of compact cadmium, one readily derives the relation $n = (1.94 \times 10^{23})R^3$. Using this relation, one obtains eq 5 from eq 2-4.

$$R = \{4\pi Nd / [(1.94 \times 10^{23}) \ln 2]\}^{1/2} C_0^{1/2} \tau_{1/2}^{1/2} \quad (5)$$

C_0 was 2.7×10^{-4} M in the experiment of Figure 6. Assuming a plausible value of $d = 10^{-5} \text{ cm}^2 \text{ s}^{-1}$ and the above half-life of 2×10^{-3} s, one obtains a mean radius R of 5.5×10^{-7} cm for the particles in the alcohol sol. Furthermore, $n = 3.3 \times 10^4$ and $[\text{Cd}_n] = 8.3 \times 10^{-9}$ M are calculated. The surface of one particle is obtained as $3.8 \times 10^4 \text{ \AA}^2$, and the total surface in 1 L as $A = 1.9 \times 10^4 \text{ cm}^2/\text{L}$ (at $C_0 = 2.7 \times 10^{-4}$ M).

In the experiments of Figure 6, $2 \times 10^{-8} \times 16 / (8.3 \times 10^{-9}) = 39$ radicals were produced per colloidal particle. When the experiments were repeated by using 64 or 256 pulses, the same half-life of the increase in conductivity was observed as in Figure 6. This shows that the rate of reaction between the radicals and colloidal particles practically did not depend on the number of electrons already transferred in the preceding pulses.

3.4. Conductivity Measurements under Continuous Irradiation. Figure 7 shows typical curves for the increase in conductivity as a function of time for various intensities of irradiation with trains of pulses of high-energy electrons.

The conductivity increase is expressed as stored electrons per liter. As mentioned in section 2.3, the concentration of stored electrons is derived from the observed increase in conductivity which is contributed by one proton formed per each stored electron. The rate J of charge transfer from the radicals to the colloidal particles is given in C/(L min) for each intensity. It is equal to the rate of radical formation multiplied by the Faraday constant.

The general features of the curves in Figure 7 resemble the ones previously observed for colloidal silver and gold solutions. The conductivity increases until the stationary state is reached. In the stationary state, the rates of charge transfer from the radicals to the colloidal particles and of the further transfer to water are equal. As soon as the irradiation ceases, the conductivity starts to decrease.

This decrease, however, is different from what has previously been observed for colloidal silver and gold solutions.^{4,5} At the higher charging rates J in Figure 7 (or higher dose rates), two distinct steps in the decrease can be recognized. The first step is similar in shape to the decrease observed earlier in studies on silver and gold. It tends to level off at 2 or 3 min after cessation of irradiation. However, it is taken over by a second rather steep decrease which first follows an almost straight line until it levels off at longer times. The final conductivity is even smaller than the one before irradiation. At the two lower charging rates J in Figure 7, where the charges stored in the stationary state are substantially smaller, the decay after irradiation seems to occur in one step. The rate of this step is equal to that of the second step at the higher charging rates. These effects show that colloidal cadmium is a more complicated storage system than the colloidal noble metals where practically only one process contributed to the discharge.

4. Discussion

4.1. Hydrogen Yield. Colloidal cadmium is as good a catalyst for the formation of hydrogen from 1-hydroxy-1-methylethyl radicals as the colloids of the noble metals. Six organic radicals are formed per 100 eV of absorbed radiation energy. Taking into account that two radicals are required to produce one molecule of hydrogen and that the radiolytically produced hydrogen peroxide ($G = 0.8/100$ eV) consumes 1.6 reduction equivalents/100 eV, one expects a maximum yield of excess hydrogen of 2.2 molecules/100 eV.¹ The observed yield is in agreement with the expectation that practically all of the generated radicals contribute to the formation of hydrogen.

At the longest irradiation time in the experiments of Figure 4, an amount of hydrogen of almost 4×10^{-2} mol had been attained in the irradiation of 1 L. As the concentration of the colloidal particles was $\sim 10^{-8}$ M, a turnover number of $\sim 4 \times 10^6$ is calculated for each cadmium particle. At this irradiation time, no decrease in catalytic activity of the formate sol was observed. In experiments with irradiation times of several weeks, a decreased yield was observed which can simply be attributed to the consumption of the 2-propanol.

4.2. Proposed Mechanism of Catalysis. 1-Hydroxy-1-methylethyl radicals do not reduce Cd²⁺ ions.⁷ The experiment of Figure 6 shows that their reaction with the colloidal particles of cadmium occurs in the time range of milliseconds, i.e., as fast as their reactions with colloidal particles of the noble metals.^{4,5} The changes in conductivity during this reaction are explained by electron transfer from the radicals to the colloidal particles (eq 1). As in the case of the noble metals, one colloidal particle may pick up electrons from several radicals. The most probable reaction of a cathodically charged cadmium

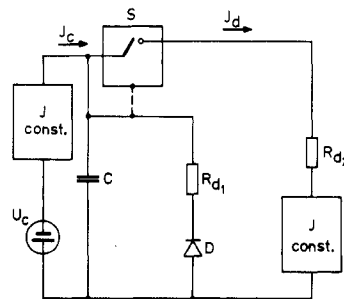
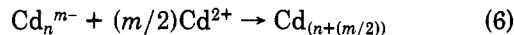
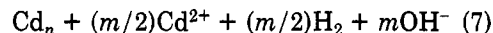
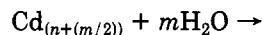


Figure 8. Equivalent electrical charging and discharging reactions of the cadmium catalyst. J_c and J_d : currents of negative charges.

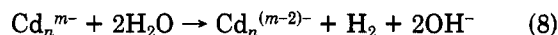
particle consists of the reduction of residual cadmium ions (eq 6, where m = number of stored electrons). The con-



centration of Cd²⁺ ions was 2×10^{-5} – 3×10^{-5} M in the experiments of Figure 7. When one applies the Nernst equation to the micrometal electrode Cd²⁺/Cd_{coll}, a potential of -0.54 V is calculated. As the cadmium atoms on the surface of a small colloidal particle have a higher chemical potential than the ones on the surface of a compact electrode, the potential may even be a little more negative. As Cd²⁺ ions are consumed in reaction 6, the potential of the microelectrode will become more and more negative. As long as cadmium ions are reduced by the transferred electrons, no excess electrons will be stored on the colloidal particles. However, reaction 6 would represent the storage of reduction equivalents, if the reduced cadmium ions were able to act as a reductant for water (eq 7). The OH⁻ ions are subsequently neutralized by protons.



We attribute the second step of the decrease in the conductivity after irradiation to this reaction (Figure 7). At low rates J of charging the microelectrode, this discharge reaction is the only step that occurs after irradiation. At high rates of charging, the concentration of residual cadmium ions will become so low that the stored electrons can finally reduce water directly (eq 8) followed by neutrali-



zation of the OH⁻ ions formed. The first step of the decrease in conductivity after completion of irradiation at a high charging rate J is attributed to this reaction. When a solution is continuously irradiated at higher dose rates, reaction 8 is responsible for the reduction of water as in the corresponding cases of the colloidal noble metals. However, when the irradiation is carried out below $\sim 10^5$ rd/h, reaction 7, i.e., electron transfer plus mass transfer of Cd from the microelectrode, must be invoked.

4.3. Equivalent Electrical Circuit. The flow of electrons to and from the microelectrode may be described by the electrical circuit of Figure 8, in which the colloid is represented by a capacitance C (in F/L). The electron transfer from the radicals is depicted as a charging current J_c that flows under the influence of a driving potential U_c . The latter may on the electrochemical scale be identified as the standard redox potential of the process



(e^- = electrons in a standard hydrogen electrode), which is close to -1.5V .⁸ J_c is constant at a given dose rate which

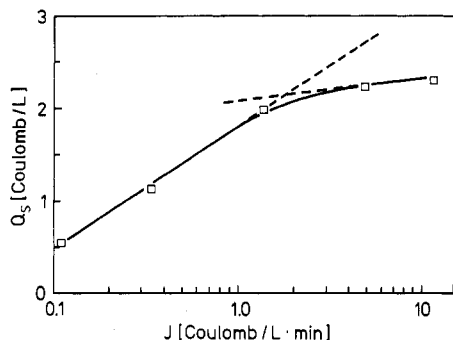


Figure 9. Reduction equivalents stored in the stationary state as a function of the rate of charging.

is described by the constant-current device on the charging side of the electrical scheme. On the discharge side of C , a distinction has to be made between reactions 7 and 8. Reaction 8 may be regarded as an electrochemical reaction whose rate depends on the stored charge Q according to eq 10, where α is the transfer coefficient of the cathodic

$$-dQ/dt = k_0 e^{\alpha n F Q / (RT C)} \quad (10)$$

reduction of water. It has previously been shown that Q as a function of t can be described by the expression $Q = A - B \ln t$, where A and B are constants.⁴ In the equivalent electrical circuit, this time behavior of the discharge current J_d is described by the resistance R_{d_1} , and the diode D . On the other hand, when reaction 7 is operative, the discharge current is almost constant over a wide range of Q . This situation is characterized by the resistance R_{d_2} in series with a constant-current device. The potential-controlled switch S puts the second mode of discharge into operation at a certain potential on C . In our further discussion, the electrical scheme will be used to define the capacity of the colloid for the storage of reduction equivalents.

4.4. Storage Capacity and Rate of Reaction 7. If the discharge reaction occurs via the electron transfer from metal to solvent (eq 8), the charge Q_s stored in the stationary state will depend on the rate J of charging according to eq 11. A semilogarithmic plot of Q_s , vs. J

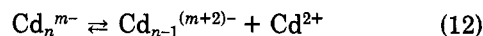
$$Q_s = RTC / (\alpha F) \ln J - \text{constant} \quad (11)$$

should yield a straight line, the slope of which is determined by the capacity C of the colloid.⁴ Figure 9 shows this plot using the data of Figure 7. It is recognized that the plot does not yield a straight line over the whole range of charging rates. In fact, one may be tempted to approximate the curve in a simplifying manner by the dashed lines obtained by extrapolation at high and low J values. The slope of the curve at high J values is 0.117 C/L. A capacity of 0.98 F/L is calculated from this slope by using $\alpha = 0.5$ in eq 11. The specific capacity C/A is obtained as $54 \mu\text{F}/\text{cm}^2$ by using $A = 1.81 \times 10^4 \text{ cm}^2/\text{L}$ (see section 3.3). This value of the specific capacity is of the order of the specific capacity of the electrical double layer of a compact metal electrode. As has been pointed out earlier, the capacity for the storage of excess electrons should be equal to the double-layer capacity provided that the immediate conversion of electrons into absorbed hydrogen atoms does not take place on a large scale.⁵ The specific capacity obtained is thus in agreement with the mechanism proposed in section 4.2 according to which the discharge occurs only via reaction 8 at high Q_s values or high J rates of charging.

The slope of the curve in Figure 9 at small J values is much greater, and an apparent specific capacity of 262

$\mu\text{F}/\text{cm}^2$ is calculated from this slope. Such a large capacity cannot be attributed to the double layer. It is best understood in terms of a charging process that does not lead to the storage of excess charges on the colloidal particles. This finding is again in agreement with the proposed mechanism of section 4.2 in which the stored charges are rapidly neutralized by the reduction of residual cadmium ions. One therefore cannot speak of the storage of charges under these conditions. However, it is still meaningful to speak of the storage of reduction equivalents (in the form of reactive Cd atoms) and to illustrate this mechanism by an equivalent electrical circuit.

As long as many excess electrons are residing on the cadmium particles, reaction 7 practically does not take place. This seems understandable as a cadmium atom at the surface of the colloid will have little tendency to leave as a cation against the Coulomb attraction of the negatively charged colloidal particle. When almost all of the excess charges have been used up for the reduction of water after irradiation, i.e., the index m in eq 8 has become small, reaction 7 will become more important. This reaction may occur in two steps:



The OH^- ions formed in reaction 13 will rapidly be neutralized. In the beginning of the discharging after irradiation, i.e. at rather low Cd^{2+} concentrations in the solution, the rate of the back-reaction is negligible. This would explain the constant rate of the second step of the discharge reaction in Figure 7. However, at higher Cd^{2+} concentration, the back-reaction of equilibrium 12 will become more important. Furthermore, the rate of reaction 13 will become lower as the Nernst potential of the system $\text{Cd}^{2+}/\text{Cd}_{\text{coll}}$ is now less negative. The leveling off of the discharge at longer times in Figure 7 is understood this way.

The slope of the linear portion of the second step in Figure 7 was $-0.45 \text{ C}/(\text{L min})$. The concentration increase of Cd^{2+} by dissolution thus was $0.45/(2F) = 2.3 \times 10^{-6} \text{ M/min}$. Using the values of $[\text{Cd}_n] = 8.3 \times 10^{-9} \text{ M}$ and $A = 1.81 \times 10^4 \text{ cm}^2/\text{L}$ (section 3.3), one obtains a rate of dissolution of $2.3 \times 10^{-6}/(8.3 \times 10^{-9}) = 277$ cadmium ions per colloidal particle per minute and an overall specific rate of dissolution of $2.3 \times 10^{-6}/(1.8 \times 10^4) = 1.2 \times 10^{-10} \text{ mol}/(\text{cm}^2 \text{ min})$.

The fact that the conductivity at long times after irradiation is even lower than that before irradiation indicates that processes are accompanying the above-described elementary steps that have not yet been recognized in detail. It should be kept in mind that the colloidal cadmium system is not in thermodynamic equilibrium, as the colloid should almost completely dissolve with time. The reduction of cadmium ions and the storage of excess electrons on the colloidal particles initiate a discharging process that finally brings the system a little closer to the thermodynamically expected state than before irradiation. Perhaps the colloidal particles are substantially changed in the storage process of eq 6; i.e., they may break apart during the deposition of additional Cd atoms. This would mean that a larger number of smaller colloidal particles are present when the dissolution process takes place after irradiation. It seems possible that such a system would approach the thermodynamically stable state more rapidly. On the other hand, the deposition of cadmium on the colloidal particles may be accompanied by the detachment of protecting polyvinyl sulfate macromolecules. The process of reabsorption of these macromolecules may re-

quire a longer time. The colloidal particles would have a larger active surface and consequently be redissolved more efficiently.

4.5. Final Conclusions. It has been shown here for the first time, that an electronegative metal can act as a catalyst in the colloidal state for the H₂ formation from radicals in aqueous solution, a domain which has generally been thought to be occupied only by the noble metals. The methods developed in the earlier work for the investigation of the mechanism of catalysis at colloidal microelectrodes were again successfully applied. The results reveal that the mechanism of catalysis is more complex in the case of cadmium than for the noble metals.

A base metal in the colloidal state may store reduction equivalents either in the form of highly reactive metal

atoms resulting from the reduction of residual ions or in the form of excess electrons. Large electron-storage capacities close to 1 F/L can be obtained as in the case of certain noble metals. It has previously been pointed out that reactions on colloidal metals can be considered as electrochemical reactions although there is no outer potential source that drives the reactions at the microelectrodes.⁹ The electrochemical description of the processes is completed in the present paper by the presentation of an analogous electrical circuit.

Acknowledgment. We thank Mrs. H. Pohl for her excellent assistance in the laboratory work.

(9) Henglein, A. *J. Phys. Chem.* 1980, 84, 3461-7.

Adsorption of Olefins on Zinc Oxide. Observations by Carbon-13 Nuclear Magnetic Resonance

Ishmall T. All and Ian D. Gay*

Department of Chemistry, Simon Fraser University, Burnaby, British Columbia V5A 1S6, Canada (Received: August 28, 1980)

A series of cyclic and acyclic olefins adsorbed on zinc oxide has been studied by ¹³C NMR. Comparison has been made with the corresponding molecules physically adsorbed on silica. In the case of olefins where the double bond is easily accessible, the chemical shifts show the presence of weak chemisorption in a π -complex bonding state. Multiple substitution of the olefinic carbons prevents the close approach of the olefin to the surface, and inhibits this mode of bonding.

Introduction

Zinc oxide is an effective catalyst for the hydrogenation¹⁻¹¹ and isomerization^{12,13,26} of olefins. Understanding of the catalytic mechanism requires an understanding of the mode of bonding of the olefin to the surface. The infrared studies of Dent and Kokes^{4-6,12,14,23} show that small olefins typically have two binding modes, which have been identified as π complexes and as π -allyl complexes. Formation of π complexes with ethylene and with propylene at high coverage has been confirmed^{15,16} by proton NMR, where the downfield shift of olefinic protons upon adsorption is readily interpreted as due to electron donation from the olefinic π bond to a surface center.

In the case of more complex molecules, such as cycloolefins¹³ the infrared studies are less clear, due to the greater complexity of the spectra, and proton NMR be-

comes unusable because of the great overlap of the broad lines which arise from adsorbed molecules of restricted mobility. It has been observed¹⁷ that ¹³C spectra of adsorbed molecules yield much more information than proton spectra, both because the lines are narrower, and because the range of chemical shifts is much greater. ¹³C spectroscopy thus suggests itself as a good means of characterizing more complex olefins adsorbed on ZnO.

Natural abundance ¹³C NMR has to date only been carried out for adsorbed species on surfaces of 200 m²/g or more, because of the unfavorable signal-to-noise ratio. The majority of the infrared and proton NMR studies have been done on Kadox-25 oxide of only 10 m²/g specific area. This difference in area creates a formidable signal-to-noise problem. We have shown¹⁸ that ZnO can be prepared from the oxalate with a higher surface area than the Kadox oxide, and with similar olefin adsorption properties. By using such an oxide, together with a wide-bore probe,¹⁹ we have been able to obtain natural abundance ¹³C spectra for a wide range of adsorbed olefins.

Experimental Section

All of the NMR spectra were measured at 25.2 MHz on a Varian XL-100 spectrometer, with TTI fourier-transform modification. Proton noise decoupling was used for all spectra. In order to study the relatively low area ZnO samples, we constructed a 22-mm probe, following the design of Zens and Grant.¹⁹ This probe produced a signal-to-noise improvement of a factor of 5 over the Varian

(1) J. F. Woodman and H. S. Taylor, *J. Am. Chem. Soc.*, **62**, 1393 (1940).

(2) E. H. Taylor and J. A. Wethington, *J. Am. Chem. Soc.*, **76**, 971 (1954).

(3) D. L. Harrison, D. Nichols, and H. Steiner, *J. Catal.*, **7**, 359 (1967).

(4) A. L. Dent and R. J. Kokes, *J. Phys. Chem.*, **73**, 3772 (1969).

(5) A. L. Dent and R. J. Kokes, *J. Phys. Chem.*, **73**, 3781 (1969).

(6) A. L. Dent and R. J. Kokes, *J. Phys. Chem.*, **74**, 3653 (1970).

(7) J. Aigueperse and S. J. Teichner, *Ann. Chim.*, **7**, 13 (1962).

(8) J. Aigueperse and S. J. Teichner, *J. Catal.*, **2**, 359 (1963).

(9) F. Bozon-Verduraz, B. Argiropoulos, and S. J. Teichner, *Bull. Soc. Chim.*, 2854 (1967).

(10) F. Bozon-Verduraz and S. J. Teichner, *J. Catal.*, **11**, 7 (1963).

(11) F. Bozon-Verduraz and S. J. Teichner, *Proc. 4th. Int. Congr. Catal.*, **85** (1968).

(12) A. L. Dent and R. J. Kokes, *J. Phys. Chem.*, **75**, 487 (1971).

(13) S. Oyekan and A. L. Dent, *J. Catal.*, **52**, 32 (1978).

(14) A. L. Dent and R. J. Kokes, *J. Am. Chem. Soc.*, **92**, 1092 (1970).

(15) A. G. Whitney and I. D. Gay, *J. Catal.*, **25**, 176 (1972).

(16) A. G. Whitney, Thesis, Simon Fraser University, 1975.

(17) I. D. Gay, *J. Phys. Chem.*, **78**, 38 (1974).

(18) I. T. All and I. D. Gay, *J. Catal.*, **62**, 341 (1980).

(19) A. P. Zens and D. M. Grant, *J. Magn. Reson.*, **30**, 85 (1978).